



Review article

Giuliana Di Martino* and Stefan Tappertzhofen^a

Optically accessible memristive devices

<https://doi.org/10.1515/nanoph-2019-0063>

Received February 27, 2019; revised April 10, 2019; accepted April 15, 2019

Abstract: One of the most promising contenders for ultralow-energy electronic devices are memristive memories, which allow for sustainably scalable “neuromorphic” computing, potentially capable of reducing power dissipation in IT by >50%. Understanding the nanoscale kinetics of the switching mechanisms is needed to enable high-endurance devices – only this can unlock their integration into fast, low-energy, logic-in-memory architectures. Lately, non-perturbative techniques were introduced to study morphological changes within memristive devices. In particular, plasmonic nanocavities recently became a smart and powerful investigation tool and opened the path for completely new electro-optical applications based on memristive devices. In this review, we will discuss the main research streams currently linking the fields of nanoscale device engineering and plasmon-enhanced light-matter interactions focusing on innovative fast ways to study real-time movement of individual atoms that underpins this new generation of ultralow-energy memory nano-devices.

Keywords: plasmonics; optical nanocavities; memristive switches; real-time spectroscopy; *in situ* spectroscopy.

1 Introduction

We are currently approaching the limit for miniaturizing transistors and memory devices using current architectures, with more and more components packed together to grow computing performance. Virtually, all power in microelectronics is converted into heat, and up to 80%

of the computing energy is consumed in the data-transfer bottleneck between logic and memory on interconnects [1], a number that will likely increase even more by further downscaling. Nowadays, IT accounts for increasing fraction (2% in 2005 and 10% in 2015) of total world energy use. Next generation high-speed microprocessors will generate heat power densities of 1000 W/cm² or more, almost similar to that emitted at the surface of the sun [2]. Cooling such devices (especially for mobile applications) will not be economically achievable. Optimization of memories or logic alone is, thus, not sufficient for sustainable power consumption. As on-chip interconnects are based on nanoscale metal wires, charging and discharging of these is time and energy consuming. To progress beyond this limit, new types of architectures are needed.

One of the most promising contenders for ultralow-energy electronic devices are resistive switching memories (RRAM), which can emulate the functionality of memristors and memristive systems. RRAMs can deliver sustainably scalable “neuromorphic” computing [3], which has the potential to reduce the energy consumption in IT by >50%. A number of fundamental studies on the working principle of memristive devices are done using electron microscopy, which is, however, destructive, invasive, and under drastically different operational conditions, so only little insight into realistic *in operando* conditions can be provided. As a result, alternative non-perturbative techniques were introduced to study morphological changes within memristive devices. In particular, the ultra-concentration of light achieved in plasmonic nanocavities became recently a smart investigation tool, overcoming the limitations of traditional investigation techniques and opening up new routes to sustainable future IT.

This review is organized in three parts. In the first part, the resistive switching mechanism is discussed with a focus on its wide range of technological applications as well as the limitations present in the current investigation techniques. The second part shows the latest progress in the field, an example of optical nanocavities, and the ability to enable optical experiments on the atomic scale. The third part links the fields of low-energy nanoscale device engineering of resistive switches and plasmon-enhanced light-matter interactions, with a close look at the RRAM potential use for optical computing.

^aNow at aixACCT Systems GmbH, Talbotstraße 25, 52068 Aachen, Germany

*Corresponding author: Dr. Giuliana Di Martino, NanoPhotonics Centre, Cavendish Laboratory, University of Cambridge, CB3 0HE, UK, e-mail: gd392@cam.ac.uk. <https://orcid.org/0000-0001-5766-8384>

Stefan Tappertzhofen: Department of Engineering, Electronic Engineering Division, University of Cambridge, CB3 0FA, UK. <https://orcid.org/0000-0003-3747-5627>

2 Resistive switching

The progressive scaling of conventional electronics is soon approaching fundamental physical limitations, and reduction in power dissipation remains the most important task in microelectronics [2]. This could be achieved if logic and memory operations were performed within the same components as more than half of the processor power is consumed by data transfer between logic and memory blocks [1]. Resistive switches are two-terminal devices, which attracted great attention due to their high scalability, ultra-fast access times, and ease of fabrication [4]. Moreover, they are one of the most promising emerging devices for logic-in-memory operations [5]. In contrast to charge-based devices, the logic states (ON and OFF) in RRAMs are encoded by the manipulation of nanoscale conductive filaments within a switching material. When a sufficiently high voltage (typically below 3 V) is applied, switching between high-resistance (HRS) and low-resistance states (LRS), to represent the logical “0” and “1”, is achieved. Migration of individual atoms can also bring quantized and multilevel resistance values, resulting in an ultrahigh-density memory device. Different types of devices exist, depending on the mobile ion species, which is responsible for the resistance transition. In this review, we will cover electrochemical metallization cells (ECM) and resistive switches based on the valence change mechanism (VCM) [6]. ECM cells are the ideal candidates for ultralow-power circuits. They consist of an active electrode, an electronically insulating, but on the nanoscale ion-conducting switching layer, and a (inert) counter electrode (Figure 1, from Ref. [7]). According to the most accepted model, a positive polarity is applied to the active

electrode (e.g. Ag) and induces an initial oxidation of the active electrode (charge-transfer reaction) and dissolution, followed by migration of Ag cations under the applied electric field. The reduction reaction at the inert electrode/solid film interface allows the nucleation process prior to filamentary growth driven by further reduction. Finally, the filament approaches the active electrode [7].

In VCM cells, the system consists of an active interface at which the switching takes place, a mixed ionic-electronic conducting layer, and an ohmic counter electrode. In the OFF-state (Figure 1, from Ref. [7]), the filament consists of the n-conducting oxide (called plug) and a potential barrier (called disc) in front of the left electrode. Upon application of a negative voltage, oxygen vacancies from the plug part of the filament are attracted into the barrier, which results in a significant decrease in the barrier height and width due to a local reduction process, which turns the cell into the ON state. For the RESET, a positive voltage is applied to the active interface, which repels the oxygen vacancies, leading to a local re-oxidation, and turns the cell into the OFF state again [7]. In VCM-based RRAMs, the comprehension of conduction mechanism is also incomplete, and the understanding through the conventional electron microscopy technique is even more challenging due to the poor material contrast (i.e. oxygen-rich and deficient regions). Various models were proposed such as filamentary conduction, charge-trapping defect states, trap-controlled space-charge-limited current, and a change of a Schottky-like barrier [8, 9]. It was suggested that electrons flow through the insulating layer by hopping along one-dimensional chains [10]. The essential feature of all of the aforementioned models is the migration of oxygen vacancies and electrons under an applied

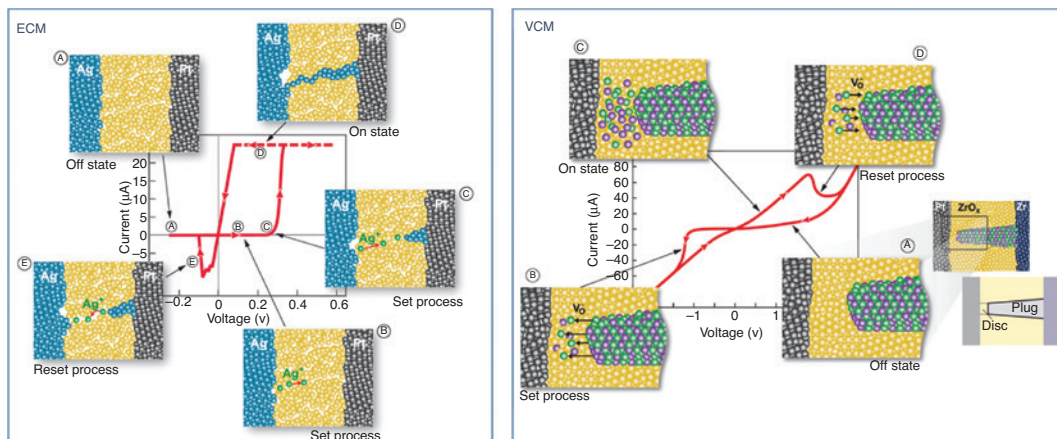


Figure 1: Typical current-voltage characteristic of an Ag/Ag-Ge-Se/Pt electrochemical metallization (ECM) and Pt/ZrOx/Zr valence change memory (VCM) cell.

Reprinted with permission from Ref. [7], Copyright 2012 John Wiley & Sons, Inc.

electric field [8]. Although VCM-based RRAMs offer a higher device endurance than ECM-RRAMs (with best results 10^{12} cycles for Ta_2O_5 -based RRAMs [11] compared to typically $<10^6$ cycles for ECM cells [12]), the programming energy of ECM cells ($\sim\text{pJ/bit}$) is about 10 times smaller than that of VCM-RRAMs [13]. Theoretical calculations predict programming energies down to 10 fJ [14], making ECM-RRAMs an ideal candidate for low-power memory-in-logic applications.

With programming energies below some pJ/bit down to fJ/bit, resistive switches become attractive for research on beyond *von Neumann* computing, where memory and logic devices are not strictly separated anymore. Within this research direction, memristive devices can be used to perform logic and memory operations in the same element(s). A first practical implementation of logic-in-memory was shown by, e.g. Heath et al. [15]. Here, the authors used a conventional memory element to control a switch that acts as a programmable interconnect. Another concept is to use memories in a passive crossbar as reconfigurable Look-Up-Tables [16]. A third concept where all necessary logic functions can be implemented using sequential logic was demonstrated by Borghetti et al. [17] in three, and later by Linn et al. [18] in a single, memristive device. In the latter study, the memristive device is at first programmed to a defined state, and at the two terminals, the logic inputs and reference voltages are then sequentially applied step-by-step according to a pre-defined scheme for each logic function. During each step, the state variable may be changed depending on the reference voltage and logic input. After the last step, the logic result is eventually stored directly in the device.

Apparently, for implementation of logic functions in memories such as resistive switches, huge improvements with respect to endurance, energy consumption, and switching speed are required to make logic-in-memory practically attractive. If the problems were solved, the advantages would be less energy consumption, smaller latencies, and more area efficiency as the number of required elements to implement logic is smaller compared to CMOS logic, and the same memory array can be used for memory and logic operations, and long interconnects can be avoided. This may be especially attractive for some applications where huge amounts of data are processed.

Device optimization is, however, limited by the poorly understood working principle of resistive switches. A number of studies have recently been published on the *in situ* characterization of the switching effect using electron microscopy [19, 20]. Apart from two studies that managed to record multiple switching cycles *in situ* [21, 22], in most of such studies [23–25], only single cycles can be observed,

and these typically differ significantly from what is observed under ambient conditions. For both ECM and VCM cells, this can be attributed to the lack of ambient oxygen and/or moisture [26, 27] involved in charge transfer reactions or ion velocity. While *in situ* TEM offers the benefit of direct observation of the filament, the sample preparation, itself, can result in stress and electric field gradients that differ significantly from realistic devices due to the cell geometry [21] or focused ion beam (FIB)-induced damage [28]. Additionally, electrons used for imaging can perturb the movement of charged metal ions during filament formation making the interpretation of these *in situ* studies difficult. Recently, the shape of filaments in RRAMs was studied by *ex situ* conductance atomic force tomography [29, 30]. This is, however, a destructive technique, dependent on not modifying the ductile filaments, and by measuring the connectedness of the sample surface to the bottom electrode, an inbuilt asymmetry is present while locally isolated filaments or particles will not be visible [29].

3 Plasmonics and optical nanocavities

The possibility to optically access the switching dynamics of memristive devices requires the understanding of the underlying concepts of how light interacts with matter leading to, i.e. the strong (“plasmonic”) field confinement on metal surfaces. When excitation of collective oscillations of electrons at interfaces (i.e. surface plasmon) is achieved, its optical properties are very sensitive to any changes in material properties, making it suitable for sensing applications. For greater light confinement, also, the lateral dimension can be reduced, leading to plasmonic waveguides with a geometry similar to standard photonic waveguides [31]. Trapping light with noble metal nanostructures overcomes the diffraction limit and can confine light to volumes typically on the order of 30 nm^3 , resulting in a further reduction of the sensing area. Coupling nanoparticles together represents a smart approach toward a large plasmonic field localization, as light can be tightly confined to the gaps between nanoparticles [32–35]. The field enhancements associated with nanoparticle clusters can also be achieved with single nanostructures separated from a metal film by a thin dielectric layer, which behave similarly to a dimer [36, 37]. Recently, fabricating nanocavities in which optically active single quantum emitters are precisely positioned became crucial for building nanophotonic devices [38]. Photon emitters placed in an optical cavity experience an environment that changes how they

are coupled to the surrounding light field [39]. With recent technological advances, coupled plasmonic nano-cavities between metallic nanostructures with sub-nm spacings became readily achievable, leading to both experimental [40–44] as well as theoretical [45–49] observations of the optical signatures of quantum mechanical effects.

In general, the alignment of the lower nanostructure facet against a flat mirror creates an ultrathin plasmonic cavity that supports multiple “cavity” resonances, defined by the geometry (or faceting) of the nanostructure on top (Figure 2, adapted from Ref. [50]). In contrast, plasmon oscillations in the nanostructure perpendicular to the surface induce image charges within the metal mirror. Plasmonic mode hybridization between tightly confined plasmonic cavity modes and a radiative antenna mode sustained in the optical nanocavities shows how optics can reveal the properties of electrical transport across well-defined metallic nanogaps to study and develop innovative technologies [50]. Strongly confined gap modes do not radiate directly, but only if they can mix with antenna modes. Modeling these systems with conducting bridges of increasing width spanning the gap shows abrupt tuning and reconfiguration of the nanogap modes [50]. Such anti-crossings are directly seen in experiments using molecular layer gap spacers, which are soft enough that optical irradiation can drive metallic nanowires between the two metal walls (Figure 3, adapted from Ref. [50]). The modes blue shift with thicker bridges because the groove cavity length L_g reduces, ejecting modes one by one from the gap [50]. The blue shifts and mode crossings, thus, allow conducting bridge diameters and locations to be determined. The model shows that field enhancement in the gap is typically three times smaller in the crevice after the gap has closed.

Even more interestingly, individual atomic features inside the gap of a plasmonic nanoassembly can localize light to volumes well below 1 nm^3 (“picocavities”), enabling optical experiments on the atomic scale [51] (Figure 4, adapted from Ref. [52]). It has been demonstrated that when such ultrasmall localization of light in these cavities is achieved, an alteration of the number

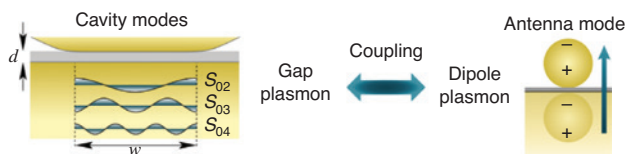


Figure 2: Schematic of the coupling between strongly confined transverse cavity modes (gap plasmon) and the radiative longitudinal antenna mode (dipole plasmon). Reprinted with permission from Ref. [50], Copyright 2016 American Chemical Society.

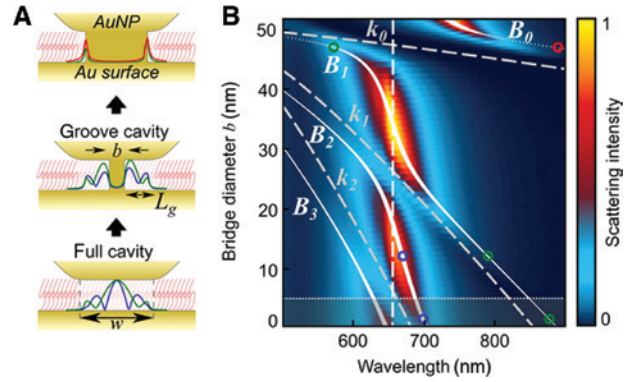


Figure 3: (A) Schematic of an NPoM with central conductive bridge linking NP and surface and (B) its corresponding finite-difference time domain simulation modes (normalized color map; yellow: high intensity, blue: low intensity). Reprinted with permission from Ref. [50], Copyright 2016 American Chemical Society.

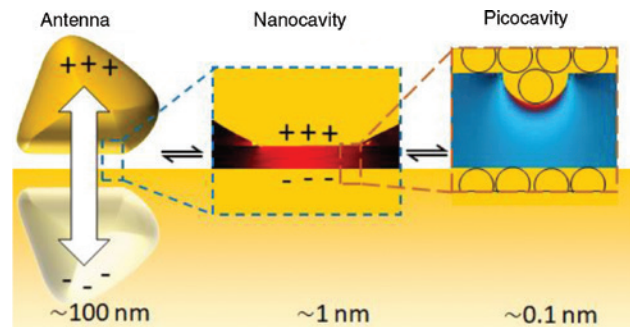


Figure 4: Effective wavelength scales between free-space photons, coupled via antennas into nanogap modes, which can then couple to atomic-scale protrusions (“picocavities”). Reprinted from Ref. [52].

and variety of vibrational modes of trapped molecules in the cavity is observed. The resulting cascaded ultrastrong plasmonic confinement pumps specific molecular bonds, thereby, creating nonthermal vibrational populations and constituting an optomechanical resonator [51]. This demonstrates the possibility of resolving the dynamics of individual bonds within molecules, which gives a sense of the power of this tool as an *in situ* investigation technique at the atomic scale.

4 Optical memristive switches

A first interaction between the light in a waveguide and the electrical resistive switching was observed in an amorphous silicon layer, where the plasmonic mode resides (Figure 5A, from Ref. [53]). The electrically triggered creation of a

metallic filament determines the variation of the absorption and scattering loss of the fundamental plasmonic mode. This results in the optical detection of an electrical RRAM switching. Similarly, it was shown that the electrically triggered addition of one atom to the filament connecting two metallic pads can result in a short circuit and a change in the electrical conductance, modifying the resonance property of the cavity (Figure 5B, from Ref. [54]). Then, in addition, an optically triggered control of atomic relocations in a metallic quantum point contact was reported [55], which demonstrates an optically controlled electronic switch based on the relocation of atoms (Figure 5C, from Ref. [55]).

Probing the electrical switching of a memristive optical antenna by electron energy loss spectroscopy (EELS) in a scanning transmission electron microscope (STEM) also showed the spatial modifications of the optical properties (LDOS) in a silver nanowire [56],

constituent of a RRAM cross-bar device (Figure 5D, from Ref. [56]).

On the other hand, these examples do not provide any spectral information in the region of the filament formation. However, ideally, optical spectroscopy would be used, instead, to give detailed information about the nanometer-scale metallic configurations exactly around the filament, itself, and the dynamics of formation and retraction [57, 58].

By integrating memristive devices as a patch antenna MIM as in Figure 6A and B, dark-field spectroscopy is capable of monitoring the real-time dynamics of the nanowire through their groove modes [58] (Figure 6A–C, adapted from Ref. [58]). The surface plasmons of the Ag-nanodot couple to their image charges in the gold film underneath the dielectric spacer layer forming a tightly confined plasmonic hotspot, similar to a nanoparticle dimer [59, 60]. The

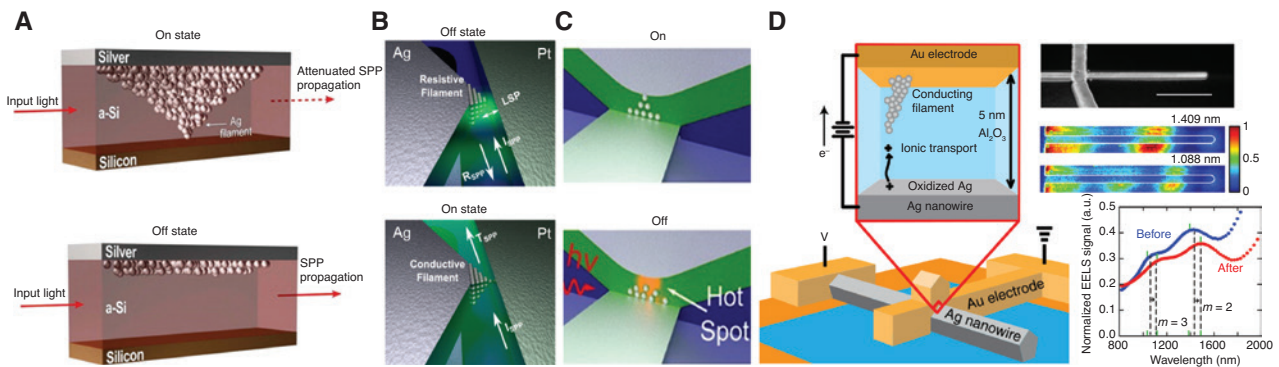


Figure 5: (A) Formation and annihilation of the nanoscale filament with optical readout functionalities, reprinted with permission from Ref. [53], Copyright 2013 American Chemical Society. (B) Interaction of incident light (ISPP) with the resistive (OFF state) and conductive (ON state) filament resulting in transmission (TSPP) and reflection (RSPP) depending on the gap distance LSP. (C) Zoom to the critical switching area. Reprinted with permission from Ref. [54], Copyright 2015 American Chemical Society from <https://pubs.acs.org/doi/abs/10.1021%2Facs.nanolett.5b04537> (further permissions related to the material excerpted should be directed to the American Chemical Society). (D) Schematic of a device for probing the electrical and optical switching properties by means of Electron Loss Spectroscopy (EELS). The zoom-in illustrates the proposed switching mechanism. The device shown in the STEM image (scale bar 400 nm) acts as an optical antenna and the switching affects the optical properties as can be seen in the STEM EELS maps and spectra. Reprinted with permission from Ref. [55] Copyright 2018 American Chemical Society, from Ref. [56] Copyright 2016 <https://creativecommons.org/licenses/by/4.0/>.

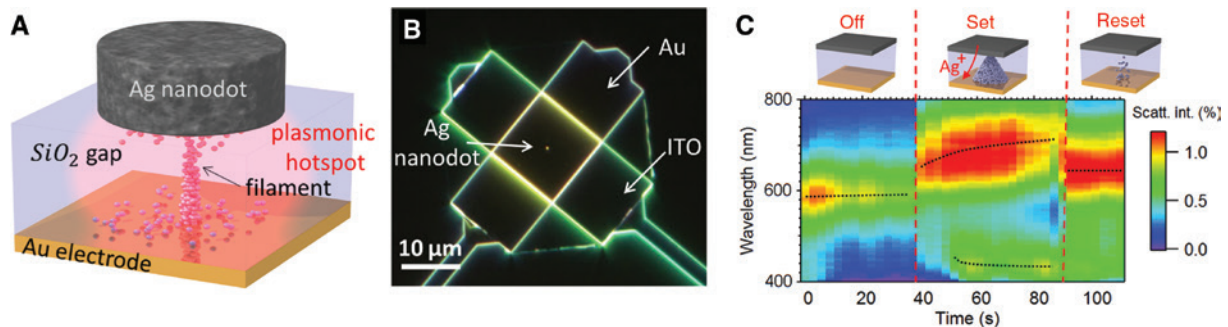


Figure 6: (A) Sketch and (B) SEM of NPoM memristive cell and (C) its optical response upon electrical switching. Reprinted with permission from Ref. [58], Copyrights 2016 by WILEY-VCH Verlag GmbH & Co. KGaA, Weinheim.

authors in Ref. [58] measured the optical response of this system by illuminating the sample with a white light beam incident at a high angle and collecting the scattered light through a dark-field objective, enabling them to follow the different phases of bridge formation within the optical nanocavity by the plasmonic mode shifts. Changes in the optical signatures allow probing morphological changes prior to the switching/forming (e.g. Figure 6C for $t < 40$ s). These changes relate to the growth and dissolution of a filament composed of only some thousands of atoms [61]. Optical characterization in such nanogaps offers a number of advantages over electron microscopy including access to *in situ* nondestructive dynamics under ambient operation conditions and realistic geometric conditions, revealing contact morphologies on the nanometer scale.

5 Potential use for optical computing

Besides heat dissipation, information transfer and processing bandwidths are limited due to electron-based charging and discharging of wires, on-chip interconnects, and terminals of logic gates. That results in a bandwidth of some tens to hundreds of GHz. In contrast, photons travel nearly loss free and all-optical devices do not suffer from charging delays. In fact, communication on inter-chip level and beyond became already the latency bottleneck for data processing, hence, the ongoing shift to optical data transmission [62]. All-optical devices have several benefits such as low crosstalk and a high potential of parallel processing [63]. Ultimately, they could replace electronic gates and fulfill the bandwidth requirements of up to 1 TB/s and beyond for future many-core architectures [64].

Most technical solutions for optical computing today are based on hybrid electro-optical devices. In Ref. [65], Sun et al. demonstrated, for example, a single-chip microprocessor that is made of a RISC-processor and photonic components. The conventional microprocessor transistors and 850 photonic components were fabricated using standard CMOS steps, demonstrating the feasibility for industrial-scale semiconductor production. With the photonic components, the chip can interact with external devices such as memory chips via optical signals. A theoretical bandwidth of 55 Gb/s could be achieved using multiple optical wavelength for data transmitting.

However, not only monolithic integration of photonics in microelectronic circuits is challenging [66] but also the bandwidth and performance of most hybrid electro-optical devices (limited due to spectral bandwidth, dispersion, or

simply because of the energy loss for converting electronic energy into photons [67]) is still only slightly better than those of conventional electronics.

Traditionally, phase-change materials were widely used in optical information processing in the past. For example, in RW-DVDs, write laser pulses induce amorphous to crystalline transitions eventually allowing for manipulation of the phase-change material's optical properties. Low-energy laser read pulses are then used to readout the encoded transmission. Phase-change materials are also used as an alternative to redox-related memristive devices as the local morphology also influences the material's electronic conductivity. Recently, chalcogenides such as $\text{Ge}_2\text{Sb}_2\text{Te}_5$ (GST) were also used as photonic memories, which can be integrated in random-access architectures [68] similar to redox-related memristive devices. A number of studies have demonstrated the implementation of photonic devices based on phase-change materials integrated in wave-guides [69–72]. In a very recent study, a GST-based photonic memory device was optically operated to perform direct scalar and matrix-vector multiplication [73]. Here, optical write pulses with energies as low as some hundreds of pJ for a few tens of ns were used to change the optical transmission within an order of magnitude in an analog way. Using a read pulse below the threshold to induce a morphological change in the material allows to multiply the non-volatily stored transmission value with the read pulse amplitude.

While research on optical interactions in phase-change materials is considerably mature, the energies for optically operated phase-change memories in the order of some hundreds of pJ are relatively high. In phase-change materials, the photonic interactions are present by mesoscopic morphological changes (crystalline vs. amorphous phases), and the potential of energy scaling is yet unknown. In contrast, in redox-based resistive switches (ECM and VCM), photons interfere with highly localized plasmonic resonances down to an almost atomic level, which may have a huge potential for further energy scaling. Emboras et al. were the first to present a redox-based memristor that can switch the optical signal during resistance transition [53] (Figure 7). The authors used an ECM-type memristor based on amorphous silicon and a silver electrode. ECM is generally considered to allow for ultralow memristive switching energies as low as some tens of fJ/bit [14]. The practical limitation of the device is the low bandwidth of their (not speed optimized) switching in the order of some kHz. A significant improvement in terms of energy and time efficiency was reported by Emboras et al. in Ref. [54]. Here, the authors demonstrated an electro-optical

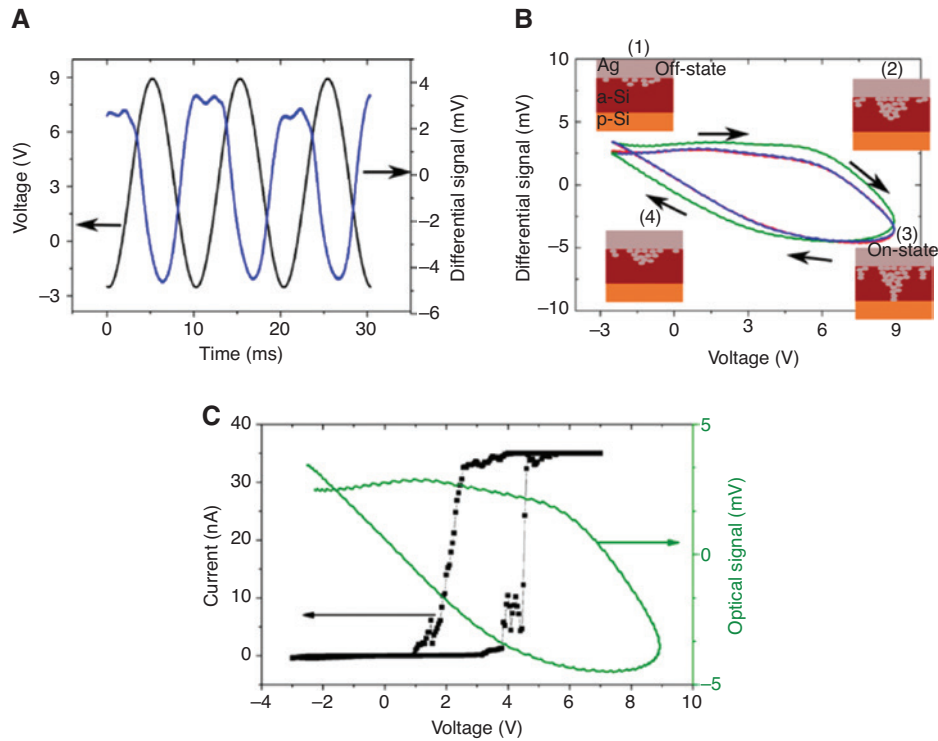


Figure 7: Modulation of an optical signal during resistive switching.

(A) A sinusoidal voltage stimulation (black) results in a modulated optical signal (here represented as a differential signal, blue). The bandwidth is limited by the resistance and capacity of the device and could be significantly improved. (B) The optical modulation is schematically contributed to the growth and rupture of a filament inside the switching insulator. (C) Resistive switching (black) characteristic versus optical signal (green).

Reprinted with permission from Ref. [53], Copyright 2013 American Chemical Society.

modulation of a silver/amorphous silicon atomic-scale plasmonic switch consuming no more than 12.5 fJ/bit. The energy consumption is, hence, competitive to conventional interconnects [1] and certainly better than the state-of-the-art LiNbO_3 Mach-Zehnder interferometer modulators, which typically operate at above 10 pJ/bit [67]. A limitation for ECM-type devices could be that their endurance (typically about 10^6 cycles [74]) is not sufficient for practical applications. VCM-type devices generally show superior endurance characteristics with a record of 10^{11} cycles [11]. An electro-optical VCM-type switch based on ZnO was demonstrated by E. Battal et al. [75]. No figure of energy consumption was provided in the study, but from the memristive hysteresis, the switching power is in the order of some tens of mW (compared to ~ 10 nW in Ref. [54]).

Although Emboras et al. could improve the operation bandwidth significantly from a few kHz to 1 MHz, the target bandwidth for practical applications is in the order of some hundreds of GHz. Nevertheless, as switching within nanoseconds was approved by several groups [11, 76, 77, 78], there is a potential of significant increase in the bandwidth.

However, the record for switching is yet in the order of some hundreds of picoseconds [79, 80] giving a bandwidth below 10 GHz; thus, significant increase in the switching speed is still required to clearly outperform competing technologies. A potential solution could be all-optically controlled resistive switches. Optically tunable switching was observed in a number of switching devices such as multiferroic [81] and ferroelectric [82] heterostructures and ferromagnets [83]. In context of memristors, an obvious practical implementation of such a device may be using photo-assisted movement of cations in chalcogenides, which was previously reported [84]. In Ref. [85], such a device where the switching can be controlled by photons is demonstrated. Here, D. Jana et al. used a thermally grown $\text{Ge}_{0.2}\text{Se}_{0.8}$ ECM-type device with Cu electrode. However, the authors used optical programming times of several seconds. In contrast, a memristor-based photodetector with an optical data throughput of 0.5 Gbit/s was demonstrated in Ref. [55] (see Figure 8). Here, the authors exploited atomic relocations in a silver metallic quantum point contact. A random bit-pattern generator (generated by digital signal processing, DSP) with an output bandwidth of 0.5 Gbit/s was used to modulate a laser

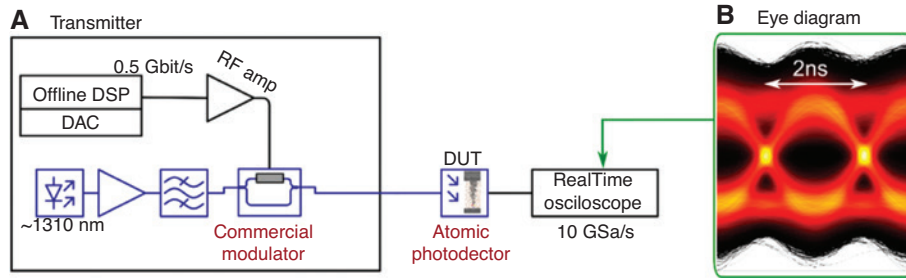


Figure 8: Experimental setup for testing 0.5 Gbit/s optical photodetection using an Ag/SiO₂/Pt device (A). (B) The experimental result is depicted showing a clear eye diagram of ~240,000 consecutive cycles. Adapted with permission from Ref. [55], Copyright 2018 American Chemical Society.

signal (1310 nm wavelength, modulated with a commercial modulator). The modulated laser signal was detected by the metallic quantum point contact ECM device. The electrical signal of the ECM device was then recorded using a high-bandwidth oscilloscope. The recorded spectrum shows an eye diagram (i.e. a transient summation of the statistically distributed signals). The vertical opening of the “eye” reveals that the transmitted signal can be successfully reconstructed. The minimum optical power required for optical switching is given as 500 nW by the authors, which results in ~1 fJ/bit.

A summary of studies demonstrating optically accessible platforms based on hybrid electro-optical devices, phase-change memories, or redox-based memristive systems is shown in Table 1. Where available, bandwidth and energy/power consumption are listed or calculated based on the experimental data of each study. It can be clearly seen that both phase-change memories and redox-based memristive device cannot yet compete in terms of bandwidth against the hybrid electro-optical approach, and further research is required to increase the bandwidth beyond 0.5 Gbit/s. However, especially ECM-based memristive devices have a huge potential in terms of energy consumption per bit.

Table 1: Comparison of the studies demonstrated optically accessible platforms for computing or memory operations based on hybrid electro-optical devices, phase change, or redox-based memristive devices.

Study	System	Bandwidth	Energy/power
[65]	Hybrid electro-optical	Up to 55 Gb/s	<0.5 pJ/bit
[73]	GST phase-change	≈100 MHz	<1 nJ/bit
[53]	ECM	Some kHz	<200 nW/bit
[54]	ECM	1 MHz	12.5 fJ/bit
[75]	VCM	n/a	<100 mW/bit
[55]	ECM	0.5 Gbit/s	1 fJ/bit

Although little is known about the optically assisted switching speed bandwidth, the potential for high bandwidth is motivated by the very nature of the switching process on the nanoscale. Though the redox processes responsible for resistance transition are still based on charge transfer (which would limit the bandwidth), the critical length for these processes was demonstrated to be in the almost atomic level [86–88]. This critical length scale makes the effective dimension where hybrid electro-optical effects are involved extremely short (and by that, the potential for high bandwidth), a far-below typical length scale that can be fabricated on industrial scale for semiconductors. In fact, the experimental data in Ref. [54] indicates electro-optical modulation based on the mass movement at a single-atom level.

6 Conclusion

This review presented the resistive switching effects and their application as the basis for future non-volatile memories. We introduced the main research streams currently linking the fields of nanoscale device engineering and plasmon-enhanced light-matter interactions. We showed the overall ability to implement optically accessible memristive switches, able to correlate the influence on the optical spectrum of the plasmonic modes present in the switching junction. In the future, it can be expected that the understanding of memristive switching mechanism will be improved, thanks to the further development of such *in situ* optical observations of the nanoscale kinetics of these switching mechanisms. With these premises, the reduction of the critical length scales down to atomic scale and the interaction of hybrid electro-optical effects will result in a new generation of ultralow-energy memory nano-devices, fundamental for sustainable future IT.

Acknowledgments: G.D.M. acknowledges support from the Winton Programme for the Physics of Sustainability and funding from ERC grant LINASS 320503, Funder Id: <http://dx.doi.org/10.13039/501100000781> and EPSRC grant EP/L027151/1, Funder Id: <http://dx.doi.org/10.13039/501100000266>. S.T. acknowledges support from DFG research fellowship under grant TA 1122/1-1 and funding from ERC grant InsituNANO 279342, Funder Id: <http://dx.doi.org/10.13039/501100000781>.

References

- [1] Miller DAB. Device requirements for optical interconnects to silicon chips. *Proc IEEE* Jul 2009;97:1166–85.
- [2] Kakac S, Vasilev LL, Bayazitoglu Y, Yener Y, Eds. *Microscale heat transfer – fundamentals and applications: proceedings of the NATO advanced study institute on microscale heat transfer – fundamentals and applications in biological and microelectromechanical systems, Cesme-Izmir, Turkey, 18–30 July, 2004*. Netherlands, Springer, 2005.
- [3] Yang JJ, Strukov DB, Stewart DR. Memristive devices for computing. *Nat Nanotechnol* 2013;8:13–24.
- [4] Yang Y Lu W. Nanoscale resistive switching devices: mechanisms and modeling. *Nanoscale* 2013;5:10076–92.
- [5] Siemon A, Breuer T, Aslam N, et al. Realization of Boolean logic functionality using redox-based memristive devices. *Adv Funct Mater* 2015;25:6414–23.
- [6] Valov I. Interfacial interactions and their impact on redox-based resistive switching memories (ReRAMs). *Semicond Sci Technol* 2017;32:093006.
- [7] Waser R. *Nanoelectronics and information technology: advanced electronic materials and novel devices*, 3rd ed. Weinheim, Germany, Wiley, 2012.
- [8] Kristof Szot RW. Redox-based resistive switching memories – nanoionic mechanisms, prospects, and challenges. *Adv Mater* 2009;21:2632.
- [9] Kim DC, Seo S, Ahn SE, et al. Electrical observations of filamentary conduction for the resistive memory switching in NiO films. *Appl Phys Lett* 2006; 88:202102.
- [10] Waser I. Resistive switching: from fundamentals of nanoionic redox processes to memristive device applications. Weinheim, Germany, Wiley, 2016.
- [11] Lee M-J, Lee CB, Lee D, et al. A fast, high-endurance and scalable non-volatile memory device made from asymmetric Ta₂O_{5-x}/TaO_{2-x} bilayer structures. *Nat Mater* 2011;10:625–30.
- [12] Kund M, Beitel G, Pinnow C-U, et al. Conductive bridging RAM (CBRAM): an emerging non-volatile memory technology scalable to sub 20 nm. In: *Electron Devices Meeting, 2005. IEDM Technical Digest. IEEE International 2005:754–7*.
- [13] Wouters DJ, Waser R, Wuttig M. Phase-change and redox-based resistive switching memories. *Proc IEEE* 2015;103:1274–88.
- [14] Ielmini D. Filamentary-switching model in RRAM for time, energy and scaling projections. In: *Electron Devices Meeting (IEDM), 2011 IEEE International 2011:17.2.1–4*.
- [15] Heath JR, Kuekes PJ, Snider GS, Williams RS. A defect-tolerant computer architecture: opportunities for nanotechnology. *Science* 1998;280:1716–21.
- [16] Paul S, Bhunia S. A scalable memory-based reconfigurable computing framework for nanoscale crossbar. *IEEE Trans Nanotechnol* 2012;11:451–62.
- [17] Borghetti J, Snider GS, Kuekes PJ, Yang JJ, Stewart DR, Williams RS. ‘Memristive’ switches enable ‘stateful’ logic operations via material implication. *Nature* 2010;464: 873–6.
- [18] Linn E, Rosezin R, Tappertzhofen S, Böttger U, Waser R. Beyond von Neumann – logic operations in passive crossbar arrays alongside memory operations. *Nanotechnology* 2012;23:305205.
- [19] Yang Y, Gao P, Li L, et al. Electrochemical dynamics of nanoscale metallic inclusions in dielectrics. *Nat Commun* 2014;5:4232.
- [20] D’Aquila K, Liu Y, Iddir H, Petford-Long AK. In situ TEM study of reversible and irreversible electroforming in Pt/Ti:NiO/Pt heterostructures. *Phys Status Solidi RRL – Rapid Res Lett* 2015;9:301–6.
- [21] Hubbard WA, Kerelsky A, Jasmin G, et al. Nanofilament formation and regeneration during Cu/Al₂O₃ resistive memory switching. *Nano Lett* 2015;15:3983–7.
- [22] Kudo M, Arita M, Ohno Y, Takahashi Y. Filament formation and erasure in molybdenum oxide during resistive switching cycles. *Appl Phys Lett* 2014;105:173504.
- [23] Liu Q, Sun J, Lv H, et al. Real-time observation on dynamic growth/dissolution of conductive filaments in oxide-electrolyte-based ReRAM. *Adv Mater* 2012;24:1844–9.
- [24] Kudo M, Arita M, Ohno Y, Fujii T, Hamada K, Takahashi Y. Preparation of resistance random access memory samples for in situ transmission electron microscopy experiments. *Thin Solid Films* 2013;533:48–53.
- [25] Choi S-J, Park G-S, Kim K-H, et al. In Situ observation of voltage-induced multilevel resistive switching in solid electrolyte memory. *Adv Mater* 2011;23:3272–7.
- [26] Tappertzhofen S, Valov I, Tsuruoka T, Hasegawa T, Waser R, Aono M. Generic relevance of counter charges for cation-based nanoscale resistive switching memories. *ACS Nano* 2013;7:6396–402.
- [27] Messerschmitt F, Kubicek M, Rupp JLM. How does moisture affect the physical property of memristance for anionic–electronic resistive switching memories? *Adv Funct Mater* 2015;25:5117–25.
- [28] *MRS Bulletin – TEM Sample Preparation and FIB-Induced Damage – Cambridge Journals Online*. [Online]. http://journals.cambridge.org/abstract_S0883769400007272. Accessed: 12 Nov 2015.
- [29] Buckwell M, Montesi L, Hudziak S, Mehonic A, Kenyon AJ. Conductance tomography of conductive filaments in intrinsic silicon-rich silica RRAM. *Nanoscale* 2015;7:18030–5.
- [30] Celano U, Goux L, Degraeve R, et al. Imaging the three-dimensional conductive channel in filamentary-based oxide resistive switching memory. *Nano Lett* 2015;15:7970–5.
- [31] Oulton RF, Bartal G, Pile DFP, Zhang X. Confinement and propagation characteristics of subwavelength plasmonic modes. *New J Phys* 2008;10:105018.
- [32] Hao E, Schatz GC. Electromagnetic fields around silver nanoparticles and dimers. *J Chem Phys* 2003;120:357–66.
- [33] Savage KJ, Hawkeye MM, Esteban R, Borisov AG, Aizpurua J, Baumberg JJ. Revealing the quantum regime in tunnelling plasmonics. *Nature* 2012;491:574–7.

- [34] Taylor RW, Esteban R, Mahajan S, Aizpurua J, Baumberg JJ. Optimizing SERS from gold nanoparticle clusters: addressing the near field by an embedded chain plasmon model. *J Phys Chem C* 2016;120:10512–22.
- [35] Myroshnychenko V, Rodríguez-Fernández J, Pastoriza-Santos I, et al. Modelling the optical response of gold nanoparticles. *Chem Soc Rev* 2008;37:1792–805.
- [36] Lévêque G, Martin OJF. Optical interactions in a plasmonic particle coupled to a metallic film. *Opt Express* 2006;14:9971–81.
- [37] Benz F, de Nijs B, Tserkezis C, et al. Generalized circuit model for coupled plasmonic systems. *Opt Express* 2015;23:33255–69.
- [38] Chikkaraddy R, Turek VA, Kongsuwan N, et al. Mapping nanoscale hotspots with single-molecule emitters assembled into plasmonic nanocavities using DNA origami. *Nano Lett* 2018;18:405–11.
- [39] Chikkaraddy R, de Nijs B, Benz F, et al. Single-molecule strong coupling at room temperature in plasmonic nanocavities. *Nature* 2016;535:127–30.
- [40] Scholl JA, García-Etxarri A, Koh AL, Dionne JA. Observation of quantum tunneling between two plasmonic nanoparticles. *Nano Lett* 2013;13:564–9.
- [41] Tan SF, Wu L, Yang JKW, Bai P, Bosman M, Nijhuis CA. Quantum plasmon resonances controlled by molecular tunnel junctions. *Science* 2014;343:1496–9.
- [42] Cha H, Yoon JH, Yoon S. Probing quantum plasmon coupling using gold nanoparticle dimers with tunable interparticle distances down to the subnanometer range. *ACS Nano* 2014;8:8554–63.
- [43] Zhu W, Crozier KB. Quantum mechanical limit to plasmonic enhancement as observed by surface-enhanced Raman scattering. *Nat Commun* 2014;5:5228.
- [44] Kravtsov V, Berweger S, Atkin JM, Raschke MB. Control of plasmon emission and dynamics at the transition from classical to quantum coupling. *Nano Lett* 2014;14:5270–5.
- [45] Zuloaga J, Prodan E, Nordlander P. Quantum description of the plasmon resonances of a nanoparticle dimer. *Nano Lett* 2009;9:887–91.
- [46] Marinica DC, Kazansky AK, Nordlander P, Aizpurua J, Borisov AG. Quantum plasmonics: nonlinear effects in the field enhancement of a plasmonic nanoparticle dimer. *Nano Lett* 2012;12:1333–9.
- [47] Esteban R, Zugarramurdi A, Zhang P, et al. A classical treatment of optical tunneling in plasmonic gaps: extending the quantum corrected model to practical situations. *Faraday Discuss* 2015;178:151–83.
- [48] Barbry M, Koval P, Marchesin F, et al. Atomistic near-field nano-plasmonics: reaching atomic-scale resolution in nanooptics. *Nano Lett* 2015;15:3410–9.
- [49] Marchesin F, Koval P, Barbry M, Aizpurua J, Sánchez-Portal D. Plasmonic response of metallic nanojunctions driven by single atom motion: quantum transport revealed in optics. *ACS Photonics* 2016;3:269–77.
- [50] Mertens J, Demetriadou A, Bowman RW, et al. Tracking optical welding through groove modes in plasmonic nanocavities. *Nano Lett* 2016;16:5605–11.
- [51] Benz F, Schmidt MK, Dreismann A, et al. Single-molecule optomechanics in ‘picocavities’. *Science* 2016;354:726–9.
- [52] Baumberg JJ, Aizpurua J, Mikkelsen MH, Smith DR. Extreme nanophotonics from ultrathin metallic gaps. *Nat Mater* 2019. <https://doi.org/10.1038/s41563-019-0290-y>.
- [53] Emboras A, Goykhman I, Desiatov B, et al. Nanoscale plasmonic memristor with optical readout functionality. *Nano Lett* 2013;13:6151–5.
- [54] Emboras A, Niegemann J, Ma P, et al. Atomic scale plasmonic switch. *Nano Lett* 2016;16:709–14.
- [55] Emboras A, Alabastris A, Ducry F, et al. Atomic scale photodetection enabled by a memristive junction. *ACS Nano* 2018;12:6706–13.
- [56] Schoen DT, Holsteen AL, Brongersma ML. Probing the electrical switching of a memristive optical antenna by STEM EELS. *Nat Commun* 2016;7:12162.
- [57] Kos D, Astier HPAG, Martino GD, et al. Electrically controlled nano and micro actuation in memristive switching devices with on-chip gas encapsulation. *Small* 2018;14:1801599.
- [58] Di Martino G, Tappertzhofen S, Hofmann S, Baumberg J. Nanoscale plasmon-enhanced spectroscopy in memristive switches. *Small* 2016;12:1334–41.
- [59] Aravind PK, Metiu H. The effects of the interaction between resonances in the electromagnetic response of a sphere-plane structure; applications to surface enhanced spectroscopy. *Surf Sci* 1983;124:506–28.
- [60] Nordlander P, Prodan E. Plasmon hybridization in nanoparticles near metallic surfaces. *Nano Lett* 2004;4:2209–13.
- [61] Menzel S, Böttger U, Waser R. Simulation of multilevel switching in electrochemical metallization memory cells. *J Appl Phys* 2012;111:014501.
- [62] Kachris C, Tomkos I. A roadmap on optical interconnects in data centre networks. In: 2015 17th International Conference on Transparent Optical Networks (ICTON), 2015:1–3.
- [63] Caulfield HJ, Dolev S. Why future supercomputing requires optics. *Nat Photonics* 2010;4:261–3.
- [64] Young IA, Mohammed E, Liao JTS, et al. Optical I/O technology for tera-scale computing. *IEEE J Solid-State Circuits* 2010;45:235–48.
- [65] Sun C, Wade MT, Lee Y, et al. Single-chip microprocessor that communicates directly using light. *Nature* 2015;528:534–8.
- [66] Orcutt JS, Moss B, Sun C, et al. Open foundry platform for high-performance electronic-photonic integration. *Opt Express* 2012;20:12222–32.
- [67] Lin H, Ogbuu O, Liu J, Zhang L, Michel J, Hu J. Breaking the energy-bandwidth limit of electrooptic modulators: theory and a device proposal. *J Light Technol* 2013;31:4029–36.
- [68] Wuttig M, Bhaskaran H, Taubner T. Phase-change materials for non-volatile photonic applications. *Nat Photonics* 2017;11:465–76.
- [69] Ikuma Y, Shoji Y, Kuwahara M, et al. Small-sized optical gate switch using Ge₂Sb₂Te₅ phase-change material integrated with silicon waveguide. *Electron Lett* 2010;46:368–9.
- [70] Kato K, Kuwahara M, Kawashima H, Tsuruoka T, Tsuda H. Current-driven phase-change optical gate switch using indium-tin-oxide heater. *Appl Phys Express* 2017;10:072201.
- [71] Stegmaier M, Rios C, Bhaskaran H, Wright CD, Pernice WHP. Nonvolatile all-optical 1×2 switch for chipscale photonic networks. *Adv Opt Mater* 2017;5:1600346.
- [72] Rios C, Hosseini P, Wright CD, Bhaskaran H, Pernice WHP. On-chip photonic memory elements employing phase-change materials. *Adv Mater* 2014;26:1372–7.
- [73] Rios C, Youngblood N, Cheng Z, et al. In-memory computing on a photonic platform. *Sci Adv* 2019;5:eaau5759.

- [74] Calderoni A, Sills S, Ramaswamy N. Performance comparison of O-based and Cu-based ReRAM for high-density applications. In: 2014 IEEE 6th International Memory Workshop (IMW) 2014:1–4.
- [75] Battal E, Ozcan A, Okyay AK. Resistive switching-based electro-optical modulation. *Adv Opt Mater* 2014;2:1149–54.
- [76] Menzel S, Tappertzhofen S, Waser R, Valov I. Switching kinetics of electrochemical metallization memory cells. *Phys Chem Chem Phys* 2013;15:6945–52.
- [77] Belmonte A, Kim W, Chan BT, et al. 90nm W\Al₂O₃\TiW\Cu 1T1R CBRAM cell showing low-power, fast and disturb-free operation. In: 2013 5th IEEE International Memory Workshop 2013:26–9.
- [78] Choi BJ, Torrezan AC, Strachan JP, et al. High-speed and low-energy nitride memristors. *Adv Funct Mater* 2016;26:5290–6.
- [79] Torrezan AC, Strachan JP, Medeiros-Ribeiro G, Williams RS. Sub-nanosecond switching of a tantalum oxide memristor. *Nanotechnology* 2011;22:485203.
- [80] Pickett MD, Williams RS. Sub-100 fs and sub-nanosecond thermally driven threshold switching in niobium oxide crosspoint nanodevices. *Nanotechnology* 2012;23:215202.
- [81] Zheng M, Ni H, Xu X, Qi Y, Li X, Gao J. Optically tunable resistive-switching memory in multiferroic heterostructures. *Phys Rev Appl* 2018;9:044039.
- [82] Li T, Lipatov A, Lu H, et al. Optical control of polarization in ferroelectric heterostructures. *Nat Commun* 2018;9:3344.
- [83] Ellis MOA, Fullerton EE, Chantrell RW. All-optical switching in granular ferromagnets caused by magnetic circular dichroism. *Sci Rep* 2016;6:30522.
- [84] El Ghrandi R, Calas J, Galibert G, Averous M. Silver photodissolution in amorphous chalcogenide thin films. *Thin Solid Films* 1992;218:259–73.
- [85] Jana D, Chakrabarti S, Rahaman SZ, Maikap S. Resistive and new optical switching memory characteristics using thermally grown Ge_{0.2}Se_{0.8} film in Cu/GeSex/W structure. *Nanoscale Res Lett* 2015;10:392.
- [86] Terabe K, Hasegawa T, Nakayama T, Aono M. Quantized conductance atomic switch. *Nature* 2005;433:47–50.
- [87] Tappertzhofen S, Valov I, Waser R. Quantum conductance and switching kinetics of AgI-based microcrossbar cells. *Nanotechnology* 2012;23:145703.
- [88] Hu C, McDaniel MD, Posadas A, Demkov AA, Ekerdt JG, Yu ET. Highly controllable and stable quantized conductance and resistive switching mechanism in single-crystal TiO₂ resistive memory on silicon. *Nano Lett* 2014;14:4360–7.